Influence of Neighboring Absorbing Receivers upon the Inter-symbol Interference in a Diffusion-based Molecular Communication System

Simon S. Assaf[1*], Shirin Salehi[1,2], Raul G. Cid-Fuentes[3], Josep Solé-Pareta[1], and Eduard Alarcón[1]
[1]NaNoNetworking Center in Catalunya (N3Cat), Universitat Politècnica de Catalunya, Spain
[2]Department of Electrical and Computer Engineering, Isfahan University of Technology, Isfahan, Iran
[3]IK4-Ikerlan Technology Research Centre, Information and Communication Technologies Area. P J.M. Arizmendiarrieta, 2. 20500 Arrasate-Mondragn, Spain
*Corresponding author: sassaf@ac.upc.edu

Abstract

A Diffusion-based Molecular Communication (DMC) system is based on the free diffusion of particles that carry the message between the transmitter and the receivers. One of the main problems which lead to decreased data rates in such network is the Inter Symbol Interference (ISI) caused by the heavy tail of the impulse response. In this paper, we study the influence of neighboring absorbing receivers upon the Inter Symbol Interference (ISI) of a Diffusion-based Molecular Communication (DMC) point-to-point link. It is shown that neighboring absorbing receivers have a noticeable impact on reducing the tail of the detected pulse-shape and, hence, higher achievable throughput are reachable.

Keywords: DMC; diffusion process; Point-to Point-link; absorbing receivers; ISI; BER; achievable throughput

1. Introduction

Nanotechnology is a very promising research field [1], and [2] . The concept of nanotechnology was first introduced in 1959 by Richard Feynman when he delivered a plenary talk entitled "There's plenty of room at the bottom". Nanotechnology enables the miniaturization and fabrication of devices in a scale ranging from 1 to 100 nanometers [3]. In other words, it is manipulation of matter on an atomic and molecular scale.

A nano-machine is composed of nano-scale components which are capable of performing simple tasks such as computing, data storing, sensing, and actuation [4]. Since the capability and functionality of a single nano-machine are

limited, nano-networks allow expanding their capabilities by establishing the communication among them.

To enable this cooperation among nano-machines, several communication mechanisms have been hitherto suggested and examined, including mechanical, acoustic, electromagnetic and molecular approaches [3]. Among these different alternative methods for interconnecting nano-machines, the bio-mimicking molecular communication case is considered to be one of the most promising mechanisms [3], in which instead of electric currents or electromagnetic waves, molecules are used to carry information from a source (transmitter) to a destination (receiver). Molecular communication is a bio-inspired paradigm where the exchange of information is realized through the transmission, propagation, and reception of molecules such as Molecular Communication via Diffusion (MCvD), ion signaling [5], active transport [6], and bacterium [7]. Among these propagation schemes, the main focus of this work will be on Diffusion-based Molecular Communication (DMC).

A DMC system consists of three main processes: emission of molecules, which is carried out by the transmitter, propagation of molecules in the medium (assuming negligible interaction among the emitted molecules [8]), where the propagation of these molecules is governed by the diffusion process. Finally, reception of molecules, which is earned out at the receivers end. In our study, the molecules are removed from the environment after hitting the receptors of the receivers (representative of biological ligand-binding mechanisms [9]). Hence, each molecule can contribute to the receiver only once; this can be modeled as the first-hitting process.

The two main research challenges of DMC are the diffusion process of molecules in the environment, which is a random process, and Inter-Symbol Interference (ISI) caused by the nature of diffusion process that leads to a heavy tail in the detected pulse shape. In other words, the reason for ISI is due to some molecules failing to arrive at the receiver end in a specific time slot, so they will interfere with the upcoming new molecules sent by the transmitter.

In the literature of DMC, first ISI has not been taken into account as in [10],[11],[12],[13],[14], and [15]. Then, in [16], and [17] the authors considered that the transmitters should not release molecules before making sure that the receivers received the intended molecules, and this is inefficient in terms of transmission rate since symbol duration will be infinite. Afterwards, some literature took into consideration the ISI effect, for example, they suggesting using incorporating ISI mitigation techniques [18],[19],[20], and [21], multiple molecules [18], and enzymes [22],[23], and [24] to reduce the ISI.

Thus, our previous work [25] it has been shown that optimal receiver distances will lead to a higher bit rate since the effect of one neighboring receiver affect the tail of the impulse response. In this paper, we focus on understanding the influence of neighboring receivers in the Inter Symbol Interference of a Diffusion-based Molecular Communication (DMC) point-to-point link. Therefore, we first model the ISI point-to-point neighboring absorbing receivers communication link, then we perform a thorough analysis by evaluating the system performance as a function of Bit Error Rate (BER) as well as achievable

throughput. Additionally, this analysis is carried out since synthetic biology is an emerging area of research that can be described as the design and construction of novel artificial biological pathways, organisms or devices, as well as the redesign of existing natural biological systems for useful purpose, for which the presented analysis can provide design oriented guidelines.

The rest of the paper is organized as follows. In section II, we introduce the system model. In section III, performance evaluation and results are shown and discussed. Finally, the conclusions are given in Section IV.

2. System model

In this section, we present the details of the emission, diffusion and reception processes while considering absorbing receivers as well as the Inter-symbol Interference (ISI) effect.

2.1. Emission and diffusion

The molecular communication system considered in this paper is a closed system in a fluid environment (such as in human body) with one transmitter and many spherical receivers disposed on the same arc circumference, as depicted in Fig. 1. Molecules are used as information carriers between the transmitter and the receiver. The receivers are located at the same distance D from the transmitter and conserve a distance d between them. The radius of the receivers is expressed as r. In addition, Fig. 1 a) shows the effect of ISI, which will be discussed in section 2.3, Fig. 1 b) displays the difference in the impulse response between the two cases, which will be elaborated in section 3.1, and finally, Fig 1 c) shows the PDF of bit zero and one which will be used to calculate the achievable throughput and the BER in section 3.3.

We consider a pulse shape modulation. In Diffusion-based Molecular Communication (DMC) the digital information is modulated in a burst of molecules if the bit is "1". Otherwise, if the bit is "0" the digital information is modulated by not releasing any molecules. Therefore, the transmitter either modulates the molecules according to an input symbol and releases a certain number of molecules at once over a time period in the medium, or it remains silent in such case the transmitter does not release any molecules. We assume that the emitted molecules are identical and indistinguishable between each other.

The molecules released by the transmitter diffuse into the medium. By neglecting the interaction among the emitted molecules [8], the dynamics of these molecules are described by Brownian motion [8] which in mathematics is described by a Wiener process as a continuous-time stochastic process. The flow of these molecules into the medium is governed by the Fick's law of diffusion. Fick's law of diffusion describes the macroscopic behavior of molecules, they estimating the concentration of molecules at any position in the medium, and it is given by [26]:

$$C\left(D,t\right)=\frac{Q}{\left(4\pi D_f\ t\right)^{3/2}}e^{-D^2/4D_f\ t} \tag{1}$$

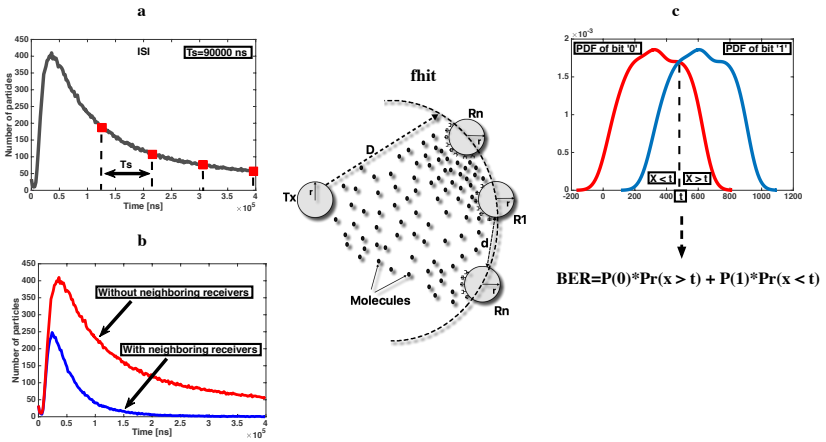

Figure 1: Considered point-to-point Diffusion-based Molecular Communication link with interfering neighboring absorbing receivers. (a) Shows the ISI effect. (b) Shows the difference between the impulse responses in both cases with and without neighboring receivers. (c) Shows the PDF of bit "0" and "1".

where D_f is the diffusion coefficient of the medium, t is time, and D is the distance from the transmitter location.

2.2. Reception process

In nature, a molecule is received by a receiver when it binds to one of the receptors on its surface. At this moment, the receiver immediately absorbs and removes the molecule from the medium through ligand-binding mechanisms [9]. Hence, after the absorption mechanism the hitting molecule can not diffuse further and hence it contributes to the signal just once.

In this work we consider absorbing receivers that are capable of counting the number of absorbed molecules at the surface of the receivers. The number of absorbed molecules over a bit interval is then demodulated as the received signal for that bit interval, where the concentration of information molecules is interpreted as the amplitude of the signal over time.

The fraction of molecules absorbed by a molecular receiver until a time t has been derived in [19] by solving the Fick's law of diffusion with two initial boundaries while taking into consideration the absorbing process.

The hitting rate of molecules f_{hit} is calculated as [19]

$$f_{hit}(t) = 4\pi r^2 R_r p(w,t|D) = \frac{r}{D}\ \frac{1}{4\pi D_f t}\ \frac{D-r}{t}\ e^{-(D-r)^2/(4D_f t)} \qquad (2)$$

where p(w,$t|D$) is the molecule distribution function, t is time, w is the distance of molecules from their initial location, D is the distance between the receivers and the transmitter with radius r, and R_r is the rate of reaction.

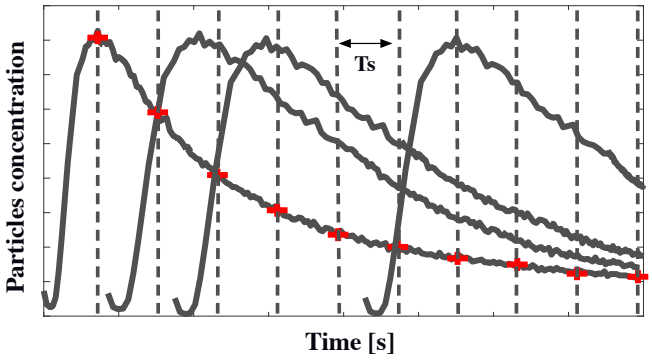

Figure 2: Effect of ISI encoded sequence.

Consequently, the fraction of molecules absorbed by the receiver F_{hit} until a given time t can be derived by integrating f_{hit} [19]

$$F_{hit}(t) = \int_0^t f_{hit}(x)dx = \frac{r}{D}\ ercf\left[\frac{D-r}{\sqrt{4D_f t}}\right] \tag{3}$$

2.3. Inter Symbol Interference (ISI)

The Inter Symbol Interference (ISI) is calculated as the time integral of the product of two output information signals which derive from two input information signals sent from a transmitter n:

$$\int_{-\infty}^{\infty} s^i_{n,out}(t) * s^{i+1}_{n,out}(t)dt \tag{4}$$

where $s^i_{n,out}(t)$ is the output information signal of the molecular communication system when the input information signal $s^i_n(t)$ is sent by the transmitter n.

Each number of molecules which represent one symbol sent by the transmitter is detected by the receivers in a time slot (T_s) called symbol duration. The molecules reaching the receivers in the following time slots present an interference source and lead to inaccurate decoding. Hence, ISI will increase when transmitting continuously molecules caused by the residual molecules from the previous symbols. Fig. 2 shows the effect of ISI across each time slot when the following binary message sequence {1,0,1,1,0,0,1} is used. Not that in the case of bit "1" the transmitter will diffuse molecules and in the case of bit "0" the transmitter will remain silent (no molecules will be released).

3. Performance evaluation and results

To assess the influence of the receivers upon the Inter-symbol Interference we apply our point-to-point link with neighboring receivers model on the open

java source simulation framework N3Sim [27], [28]. N3Sim is a complete simulation framework for diffusion-based molecular communications, which allows the evaluation of the communication performance of molecular networks with several transmitters and receivers mimicking an infinite space with a given concentration of molecules. Accordingly, this simulator allows us to encode the information in the transmitters by diffusing particles into the medium, a diffusion of particles through the medium which is modeled as Brownian motion, and finally, receivers decode the information by detecting and absorbing the local concentration in their surrounding environment.

Therefore, we evaluate the performance of the communication via diffusion system by using neurotransmitters as the messenger molecules which diffuse in the chemical synaptic cleft to exchange information between two neurons [29]. Hence, the performance evaluation is carried out using GABA particles as the messenger molecule and, as the receiver, a device whose parameters are similar to a $GABA_A$ receptor with a fixed radius r equal to 4 nm [30]. D represents the distance of the chemical synaptic cleft and it is equal to 20 nm [29]. By disposing the receivers on the same arc circumference, the number of receivers varies from three to nineteen where d equals 1 nm. For d equal to 20 nm the number of receivers varies from three to fifteen, however, for d equal to 60 nm the number of receivers varies from three to seven. The simulation time is set to 40 μs, with a time-step of 0.2 μs. The number of released molecules is fixed to 500000 molecules. Note that the choice of the simulation parameters is in nanometre range since the Diffusion-based Molecular Communication (DMC) is expected to be suitable for covering short distances from nanometer to micrometer (nm - μm).

Please refer to the appendix for a short tutorial section on how to simulate SIMO MOLCOM scenarios in N3Sim.

3.1. Impulse response

Fig. 3 shows the set of the impulse responses at receiver one (R_1) with a different number of receivers (3, 7, 11, 15, and 19 receivers) where d equal to 1 nm in Fig. 3 a), 20 nm in Fig. 3 b), and 60 nm in Fig. 3 c). This set of impulse responses is compared to the ideal pulse-shape where receiver one (R_1) resides alone without any neighboring receivers. The influence of the neighboring receivers upon the pulse-shape affects first the maximum amplitude reached by the ideal case, by decreasing as the number of receiver increase. Second, the amplitude of the tail shows a significant reduction, as the number of neighboring receivers increases till it reaches zero as T_s increase. The increase of d leads to a decrease of the number of relevant receivers, hence, the amplitude of the tail as well as the maximum amplitude, thereby approaching that of the ideal impulse response case.

3.2. Normalized amplitude, pulse energy and pulse width

In Fig. 4 we show the impact of the neighboring receivers as a function of amplitude, pulse energy, and pulse width on the impulse response of receiver

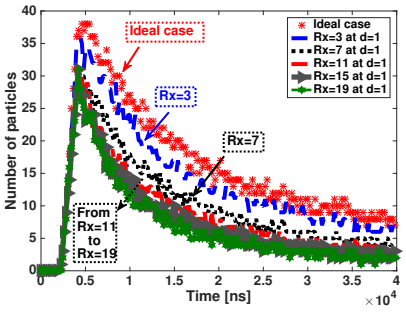

(a) d equal to 1 nm.

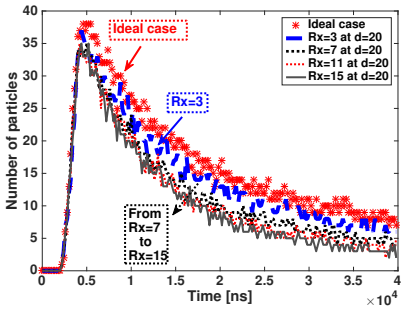

(b) d equal to 20 nm.

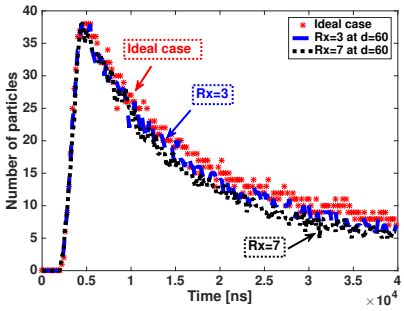

(c) d equal to 60 nm.

Figure 3: Set of impulse responses at receiver one R1 for different numbers of receivers where d equal to 1, 20, and 60 nm and D is fixed to 20 nm.

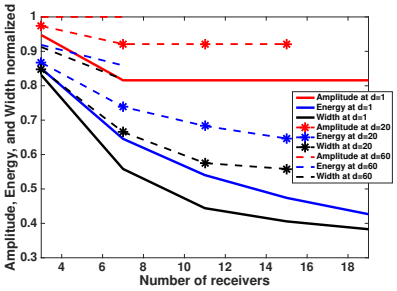

Figure 4: Pulse amplitude, width and energy at receiver one R_1 for different numbers of receivers where d equal to 1, 20, and 60 nm and D is fixed to 20 nm.

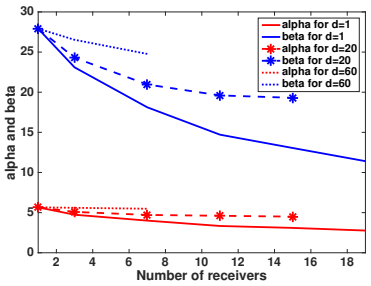

Figure 5: Linear model at receiver one R_1 for different numbers of receivers where d equal to 1, 20, and 60 nm and D is fixed to 20 nm.

one (R_1). The number of receivers varies from three to nineteen where d equals 1 nm. For d equal to 20 nm the number of receivers varies from three to fifteen, however, for d equal to 60 nm the number of receivers varies from three to seven. Note that D is fixed to 20 nm.

As we can see, the pulse energy and the pulse width of the detected pulse-shape decrease as the number of receivers increase for the different values of d. In particular, the pulse width and the pulse energy decrease approximately 45 % and 43 % respectively from three to nineteen receivers for the cases where d equal to 1 nm. However, the pulse width and the pulse energy decrease approximately 29 % and 22 % respectively from three to fifteen receivers for the cases where d equal to 20 nm. On the other hand, when d equal to 60 nm, the pulse width and the pulse energy decrease approximately 10 % and 6 % respectively from three to seven receivers. Besides, in the case where d equal to 1 nm, and 20 nm the amplitude of the impulse response at receiver one R_1 reaches its steady state after nine receivers even if we increase the number of receivers, since only receiver two (R_2) to receiver nine (R_9) have an impact on the maximum amplitude of the impulse response at receiver one (R_1). However, in the case where d is equal to 60 nm the amplitude of the impulse response at receiver one R_1 will remain the same since the effect of neighboring receivers will diminish at this distance.

Accordingly, as d is smaller, the neighboring receivers are able to absorb more molecules in front of receiver one (R_1), hence showing a significant reduction on the pulse amplitude, pulse width and pulse energy. For fixed pulse amplitude, lower pulse energy and width imply lower pulse time and, hence, higher bit rates.

As it shown in Fig. 3 and 4, after the amplitude reaches it is maximum, the tail of the impulse response is varying as a polynomial decay when we increase the number of receivers. Fig. 5 shows the linear model at d equal to 1, 20, and 60 nm. First, we model the decay of the pulse by

$$\left(\frac{Q}{(t)}\right)^{\alpha} \tag{5}$$

where Q represents the number of molecules released and t is the time.

Then, we calculate these parameters as a logarithmic function

$$Y = \left(\frac{\beta}{(t)^{\alpha}}\right) \tag{6}$$

$$\log(Y) = \log(Q) - \alpha \log(t) \tag{7}$$

Finally, the linear model is calculated as

$$f(x) = p_1 x + p_2 \tag{8}$$

where α = - $p_1 10^{-4}$ and $\beta = p_2$

Therefore, by knowing the maximum reached amplitude, we can reconstruct the tail of the impulse response. Hence, by reconstructing the tails of the impulse response we calculated in section 3.3 the achievable throughput and the BER reached at each specific case.

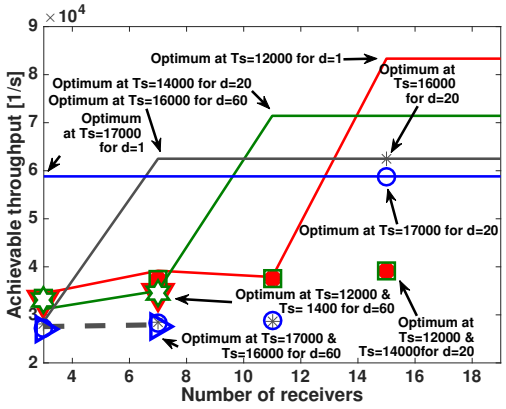

Figure 6: Achievable throughput as a function of number of receivers where d = 1, 20, and 60 nm. Number of receivers for d equal to 1 nm varies from 1 to 19. Number of receivers for d equal to 20 nm varies from 3 to 15. Number of receivers for d equal to 60 nm varies from 3 to 7.

3.3. Achievable throughput and BER

Fig. 6 displays the achievable throughput at receiver one (R_1) as a function of the number of receivers as well as a function of time slot (T_s). The number of receivers varies from three to nineteen where d equal to 1 nm. For d equal to 20 nm the number of receivers varies from three to fifteen, however, for d equal to 60 nm the number of receivers varies from three to seven. First, the achievable throughput increases as the number of receivers increase till it reaches the optimum value for each T_s. This shows a good effect for neighboring absorbing receivers. However, no similar trend is obtained when we increase the number of receivers after the optimum values are reached, since the achievable throughput will remain the same, hence as the number of receivers increase the achievable throughput will be the same after reaching its maximum for each T_s. Second, as we can see when d is equal to 1 nm the achievable throughput reaches the maximum, since the effect of neighboring absorbing receivers at receiver one (R_1) is high at this distance d. However, no similar trend is shown when we increase d since the effect of neighboring receivers at receiver one (R_1) will diminish. Therefore, as the number of neighboring receivers increase, the achievable throughput will be higher for the same T_s.

In Fig. 7 we illustrate the achievable throughput at receiver one (R_1) as a function of time slot (T_s) where d equal to 1 nm in Fig. 7 a), 20 nm in Fig. 7 b), and 60 nm in Fig. 7 c). These achievable throughputs are compared to the ideal achievable throughput where receiver one (R_1) resides alone without any neighboring receivers. First, in Fig 7 a) and b) the result shows the positive influence of the neighboring receivers upon the achievable throughput. In the ideal case the optimum achievable throughput is approximately equal to 33380 bits/s however, it reaches approximately 83330 bits/s and 62500 bits/s in the case where we have fifteen neighboring absorbing receivers and d equal to 1, and

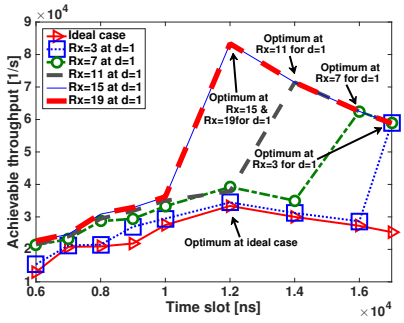

(a) d equal to 1 nm.

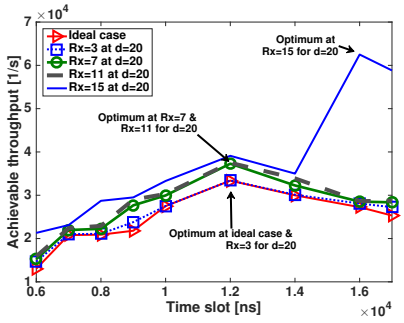

(b) d equal to 20 nm.

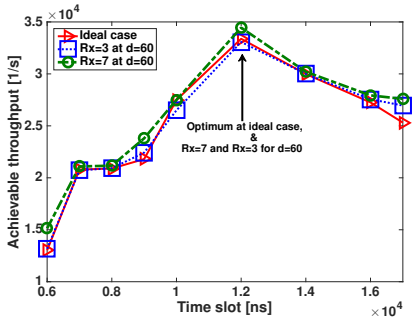

(c) d equal to 60 nm.

Figure 7: Achievable throughput as a function of T_s where $d = 1$, 20 and 60 nm. Number of receivers for d equal to 1 varies as 3, 7, 11, 15, and 19. For d equal to 20 nm the number of receivers is equal to 3, 7, 11, and 15. For d equal to 60 nm the number of receivers is equal to 3 and 7.

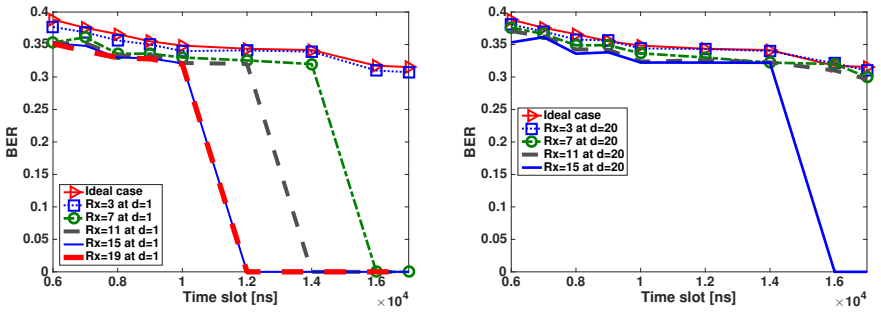

(a) d equal to 1 nm.

(b) d equal to 20 nm.

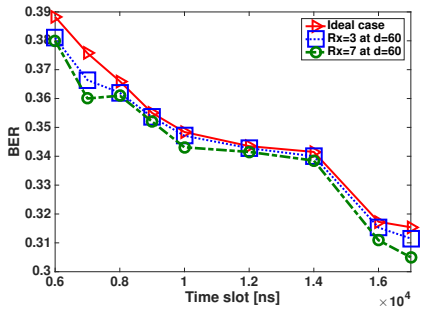

(c) d equal to 60 nm.

Figure 8: Bit Error Rate as a function of T_s where where $d = 1$, 20 and 60 nm. Number of receivers for d equal to 1 varies as 3, 7, 11, 15, and 19. For d equal to 20 nm the number of receivers is equal to 3, 7, 11, and 15. For d equal to 60 nm the number of receivers is equal to 3 and 7.

20 nm respectively. However, in Fig. 7 c) the optimum achievable throughput is approximately the same as the ideal case. Hence, at this distance d the effect of neighboring receivers on receiver one (R_1) will become negligible. In addition, the optimum achievable throughput at seven absorbing receivers decreases from 62500 bits/s at d equal to 1 nm to 34550 bits/s at d equal to 60 nm. Therefore, as d is smaller, the influence of the neighboring receivers upon receiver one (R_1) will be stronger, which leads to a higher achievable throughput. Second, when we increase the number of T_s and after the optimum values are reached, the achievable throughput will be equal to the bit rate, hence as T_s increase the achievable throughput will decrease after reaching its maximum.

In Fig. 8 we show the Bit Error Rate (BER) as a function of Time slot (T_s) where d equal to 1 nm in Fig. 8 a), 20 nm in Fig. 8 b), and 60 nm in Fig. 8 c). These Bit Error Rates are compared to the ideal BER where (R_1) reside alone. First, the result reveals that as T_s and number of receivers increase the BER will decrease until it reaches zero. For example, in the case where we have fifteen receivers for d equal to 1 nm and T_s is larger than 12000 ns, the BER will be zero. Second, in Fig. 8 a) at fifteen absorbing receivers the BER reaches zero when T_s is larger than 12000 ns, however, in Fig. 8 b) the BER reaches zero at T_s larger than 16000 ns. Hence, as d is smaller the BER reaches zero at a smaller T_s. Moreover, in Fig. 8 c) we can see that even if we increase the number of receivers the BER will remain approximately the same as in the ideal case. Hence, at this distance d there is no effect of neighboring receivers on receiver one (R_1).

From the last two plots we see that as the tail of the impulse response goes to zero at a specific number of receivers and specific T_s, the BER will go to zero and the achievable throughput will reach its maximum. In such case, the effect of ISI in the system is canceled. Note that for a smaller d the tail of the impulse response will change steeper to zero and, hence, better achievable throughput is reached. However, as T_s increases the maximum achievable throughput will decrease since we are increasing the symbol duration, which leads to inefficiency in terms of transmission rate.

4. Conclusion

In this paper, a simplified MOLCOM synthetic scenario valuable for a design space exploration, yet representative of practical deployments where the position of each receiver is on the same arc circumference is studied. It has been shown that the optimal number of neighboring absorbing receivers and the optimal distance d between the receivers leads first to a steady state in the maximum amplitude of the impulse response and cancel the effect of ISI by reducing the amplitude of the tail. Therefore, in such case lower BER as well as a higher achievable throughput will be reached. In the same orientation, in our future work the Single Input Multiple Output (SIMO) will be investigated.

Appendix

First, the only prerequisite to install the jar file N3Sim.cfg and the configuration file N3Sim.cfg is Java JRE 1.6. These files can be found at the N3cat web site (http://www.n3cat.upc.edu).

In the configuration file, we can classify and organize the parameters as follows: Simulation parameters, space parameters, emitter parameters, and finally receivers parameters.

For the simulation parameters we can specify the name of the folder where the result files will be stored, the value of the particle displacements due to Brownian motion (default set to 1), the collision among the emitted particles (if set to false the emitted particles are assumed to be transparent to each other and never collide), the total time of the simulation as well as the duration of each time step.

In the space parameter we can define for example if the system is bounded or unbounded (for the bounded system a rectangular bounded space is simulated where you need to specify his coordinates X and Y), the diffusion coefficient, and the radius of the emitted particles.

In the emitter parameters we can indicate the number of transmitters, the transmitter's radius, the transmitter's location (horizontal and vertical location), the release particles time with their initial speed, the number of particles released by the transmitter at every time step, and the type of the transmitter (Type one where the transmitters emits a fixed number of particles at every time step, type two where the transmitter emits particles following rectangular waveform, type three where the transmitter emits particles following a white noise waveform, type four where the transmitters reads the waveform of the signal to be emitted from a text file, and finally type five where the transmitters is the same as transmitter type four but in a 3-dimensional simulation space).

For the receiver parameters we can indicate the number of receivers, the receiver's radius, the receiver's location (horizontal and vertical location), the receiver's name, and the receivers type (Type one where the detection area of the receiver is a square, type two where the detection area of the receiver is a circle, type three where the detection volume of the receiver is a sphere).

Note that the units of the parameters are nanometers (nm) and nanoseconds (ns).

SIMO stands for Single Input Multiple Output where we have single transmission node and multiple reception nodes from the same information sink. Hence, to simulate a SIMO MOLCOM scenarios used in this paper for SISO with adjacent absorbing receivers we need to specify in the configuration file mentioned above the following parameters:

1. The number of transmitters: Set to one.
2. The location of the transmitter and its radius.
3. The start time and the end time of releasing particles.
4. The type of transmitters.
5. The number of released particles.

6. The number of receivers: Set to two or higher.
7. The name of each receivers.
8. The location of the receivers: The receivers should maintain the same distance from the transmitters so the receivers are disposed on the same arc circumference.
9. The type of receivers.
10. The radii of the receivers.
11. The distance between the transmitter and the receivers.
12. The distance between the receivers.

After editing the values of the parameters in the downloaded configuration file (N3Sim.cfg) in order to have a specific SIMO MOLCOM scenario, we need to write the following console command to start the simulation process:

- java -jar N3Sim-0.7.jar myConfigFile.cfg

Finally, when the simulation is ended, we can find a file under the name of `receiver_name.csv` for each receiver in the simulation. The output of these files can be divided into two columns, the first column contains the time steps in nanoseconds, and the second one represents the number of particles measured by the receiver at the each time step.

Acknowledgements

This work was partially supported by 1) the Catalan Government under the contract 2014SGR-1427, and 2) the aid granted by the Spanish Ministry of Science and Innovation under the project SUNSET (FEDER-TEC 2014-59583-C2-2-R). Also this work has been done under the framework of the CIRCLE project (H2020-CSA-665564) funded by the EU.

References

[1] N. Farsad, H. B. Yilmaz, C. B. Chae A. W. Eckford, , and W. Guo. A comprehensive survey of recent advancements in molecular communication. *IEEE Communication Surveys Tuts*, 18(3):1887–1919, 2016.

[2] T.Nakano, A. W. Eckford, and T. Haraguchi. Molecularcommunication. *Cambridge University Press*, 2013.

[3] I. F. Akildiz, F. Brunetti, and C. Blazquez. Nanonetworks: A new communication paradigm. *Elsevier Computer Networks*, 52(12):2260–2279, August 2008.

[4] T. Suda, M. Moore, T. Nakano R. Egashira, and A. Enomoto. Exploratory research on molecular communication between nanomachines. *Proc. Genetic and Evolutionary Computation Conference*, June 2005.

[5] M. S. Kuran, T. Tugcu, and B. O. Edis. Calcium signaling: Overview and research directions of a molecular communication paradigm. *IEEE Wireless Communications*, 19(5):20–27, October 2012.

[6] S. Hiyama, R. Gojo, T. Shima, S. Takeuchi, and K. Sutoh. Biomolecular motor based nano or microscale particle translocations on dna microarrays. *Nano Letters*, 9(6):2407–2413, April 2009.

[7] P. Lio and S. Balasubramaniam. Opportunistic routing through conjugation in bacteria communication nanonetwork. *Elsevier Nano Communication Networks*, 3(1):36–45, March 2012.

[8] I. Karatzas and S. E. Shreve. *Brownian Motion and Stochastic Calculus*. Springer, 1991.

[9] J. Rospars, V. K rivan, and P. Lánský. Perireceptor and receptor events in olfaction. comparison of concentration and flux detectors: a modeling study. *Chem. Senses*, 5(3):293–311, June 2000.

[10] S. Kadloor and R. Adve. A framework to study the molecular communication system. *Proc. IEEE ICCCN*, pages 1 – 6, August 2009.

[11] A. Einolghozati, M. Sardari, A. Beirami, , and F. Fekri. Capacity of discrete molecular diffusion channels. *Proc. 2009 IEEE ISIT*, pages 723 – 727, August 2011.

[12] S. Kadloor, R. R. Adve, and A. W. Eckford. Molecular communication using brownian motion with drift. *Trans. Nanobiosci*, 11:89 – 99, June 2012.

[13] K. V. Srinivas, A. W. Eckford, and R. S. Adve. Molecular communication in fluid media: The additive inverse gaussian noise channel. *IEEE Trans. Inf. Theory*, 58:4678 – 4692, July 2012.

[14] T. Nakano, Y. Okaie, and A. V. Vasilakos. Throughput and efficiency of molecular communication between nanomachine. *IEEE WCNC*, pages 704 – 708, April 2012.

[15] K. C. Chen L. S. Meng, P.-C. Yeh and I. F. Akyildiz. Mimo communications based on molecular diffusion. *Proc. IEEE GLOBECOM*, pages 5602 – 5607, December 2012.

[16] M. Pierobon and I. F. Akyildiz. Inter symbol and co-channel interference in diffusion-based molecular communication. *Proc. IEEE ICC MONACOM*, pages 6126 – 6131, June 2012.

[17] M. S. Leeson and M. D. Higgins. Forward error correction for molecular communications. *Nano Commun. Net.*, pages 161 – 167, September 2012.

[18] H. B. Yilmaz and C. Chae. Simulation study of molecular communication systems with an absorbing receiver: Modulation and isi mitigation techniques. *Simul. Model. Pract. Theory*, 49:136 – 150, December 2014.

[19] B. Tepekule, A E. Pusane, C. Chae H. Birkan Yilmaz, and Tuna Tugcu. Isi mitigation techniques in molecular communication. *IEEE transaction on molecular*, pages 2332 – 7804, June 2015.

[20] M. U. Mahfuz, D. Makrakis, and H. T. Mouftah. Performance analysis of convolutional coding techniques in diffusion-based concentration-encoded pam molecular communication systems. *Springer Bio-NanoSci.*, 3(3):270–284, September 2013.

[21] P. J. Shih, C. H. Lee, P. C. Yeh, and K. C. Chen. Channel codes for reliability enhancement in molecular communication. *IEEE J. Sel. Areas Communication*, 31(12):857–867, December 2013.

[22] A. Noel, K. Cheung, and R. Schober. Improving receiver performance of diffusive molecular communication with enzymes. *IEEE Trans. Nanobioscience*, 13:31 – 43, MARCH 2014.

[23] Y. J. Cho, H. B. Yilmazand, W. Guo, and C. B. Chae. Effective intersymbol interference mitigation with a limited amount of enzymes in molecular communications. *Wiley Trans. Emerging Telecommunication*, September 2016.

[24] N. Farsad, H. B. Yilmaz, C. B. Chae A. W. Eckford, , and W. Guo. Interference reduction via enzyme deployment for molecular communication. *IET Electron. Lett.*, 52(13):1094–1096, June 2016.

[25] S. S. Assaf, S. Salehi, R. G. Cid-Fuentes, J. Solé-Pareta, and E. Alarcón. Characterizing the physical influence of neighboring absorbing receivers in molecular communication. *NANOCOM*, 42, September 2016.

[26] W. H. Bossert and E. O. Wilson. The analysis of olfactory communication among animals. *Theoretical biology*, 5(3):443–469, November 1963.

[27] I. Llatser, D. Demiray, A. C. Aparicio, D. T. Altilar, and Alarcón. N3sim: Simulation framework for diffusion-based molecular communication nanonetworks. *Simul. Model. Practice Theory*, 42:210–222, March 2014.

[28] N. Garralda, I. Llatser, C. Aparicio, and M. Pierobon. Simulation-based evaluation of the diffusion-based physical channel in molecular nanonetworks. *Proc. of the 1st IEEE International Workshop on Molecular and Nano Scale Communication (MoNaCom)*, April 2011.

[29] E. R. Kandel, J. H. Schwartz, and T. Jessell. Principles of neural science. *McGraw-Hill, New York, ed. 4*, 2000.

[30] P. S. Miller and A. R. Aricescu. Crystal structure of a human $gaba_a$ receptor. *Nature*, pages 270–275, August 2014.